

Stochastic fluctuations of bosonic dark matter

Gary P. Centers^{1,2}, John W. Blanchard², Jan Conrad³, Nataniel L. Figueroa^{1,2}, Antoine Garcon^{1,2}, Alexander V. Gramolin⁴, Derek F. Jackson Kimball⁵, Matthew Lawson^{2,3}, Bart Pelssers³, Joseph A. Smiga^{1,2}, Alexander O. Sushkov⁴, Arne Wickenbrock^{1,2}, Dmitry Budker^{1,2,6,*}, and Andrei Derevianko⁷

¹*Johannes Gutenberg-Universität, Mainz 55128, Germany*

²*Helmholtz Institute, Mainz 55099, Germany*

³*Department of Physics, Stockholm University, AlbaNova,10691 Stockholm, Sweden*

⁴*Department of Physics, Boston University, Boston, Massachusetts 02215, USA*

⁵*Department of Physics, California State University East Bay, Hayward, California 94542-3084, USA*

⁶*Department of Physics, University of California, Berkeley, CA 94720-7300, USA*

⁷*Department of Physics, University of Nevada, Reno, Nevada 89557, USA and*

**Corresponding Author, Email: budker@uni-mainz.de*

(Dated: May 12, 2022)

Numerous theories extending beyond the standard model of particle physics predict the existence of spin-0 bosons [1–11] that could constitute the dark matter (DM) permeating the universe. In the standard halo model (SHM) of galactic dark matter the velocity distribution of the bosonic DM field defines a characteristic coherence time τ_c . Until recently, laboratory experiments searching for bosonic DM fields have been in the regime where the measurement time T significantly exceeds τ_c [12–26], so null results have been interpreted as constraints on the coupling of bosonic DM to standard model particles with a bosonic DM field amplitude Φ_0 fixed by the average local DM density. However, motivated by new theoretical developments [27–32], a number of recent searches [33–39] probe the regime where $T \ll \tau_c$. Here we show that experiments operating in this regime do not sample the full distribution of bosonic DM field amplitudes so results cannot assume a fixed value of Φ_0 . Instead, in order to interpret laboratory measurements (even in the event of a discovery), it is necessary to account for the stochastic nature of such a virialized ultralight field (VULF) [40–42]. Re-examining previous null experiments in the context of stochastic DM fluctuations shows that at least seven published constraints are overestimated by roughly one order of magnitude.

It has been nearly ninety years since strong evidence of the missing mass we label today as dark matter was revealed [43], and its composition remains one of the most important unanswered questions in physics. There have been many DM candidates proposed and a broad class of them, including scalar (dilaton and moduli [1–4]) and pseudoscalar particles (axions and axion-like particles [5–11]), can be treated as an ensemble of identical spin-0 bosons whose statistical properties are described by the SHM [44, 45]. In this work, our model of the resulting bosonic field assumes that the local DM is virialized and neglects non-virialized streams of DM [46], Bose-Einstein

condensate formation [47–49], and possible small-scale structure such as miniclusters [50, 51].

During the formation of the Milky Way these DM constituents relax into the gravitational potential and obtain, in the galactic reference frame, a velocity distribution with a characteristic dispersion (virial) velocity $v_{\text{vir}} \approx 10^{-3}c$ and a cut-off at the galactic escape velocity. For particle masses $m_\phi \ll 10 \text{ eV}$ the average mode occupation numbers of the DM field are large enough such that it may be treated as a classical field.

Following Refs. [40–42] we refer to such virialized ultralight fields, $\phi(t, \mathbf{r})$, as VULFs, emphasizing their SHM-governed stochastic nature. Neglecting motion of the DM, the field oscillates at the Compton frequency $f_c = m_\phi c^2 h^{-1}$. However, there is broadening due to the SHM velocity distribution according to the dispersion relation for massive nonrelativistic bosons: $f_\phi = f_c + m_\phi v^2 (2h)^{-1}$. The field modes of different frequency and random phase interfere with one another resulting in a net field exhibiting stochastic behavior. The dephasing of the net field can be characterized by the coherence time ¹ $\tau_c \equiv (f_c v_{\text{vir}}^2 / c^2)^{-1}$.

While the stochastic properties of similar fields have been studied before, for example in the contexts of statistical radiophysics, the cosmic microwave background, and stochastic gravitational fields [52], the statistical properties of VULFs have only been explored recently. The 2-point correlation function, $\langle \phi(t, \mathbf{r}) \phi(t', \mathbf{r}') \rangle$, and corresponding frequency-space DM “lineshape” (power spectral density, PSD) were derived in Ref. [41], and red-erived in the axion context by the authors of Ref. [53]. References [41, 53] explicitly discuss data-analysis implications only in the regime of the total observation time T being much larger than the coherence time, $T \gg \tau_c$. However, investigation of the regime $T \ll \tau_c$ has been

¹ We note that there is some ambiguity in the definition of the coherence time, up to a factor of 2π , and adopt that which was used in the majority of the literature. See the discussion in the Supplementary Material.

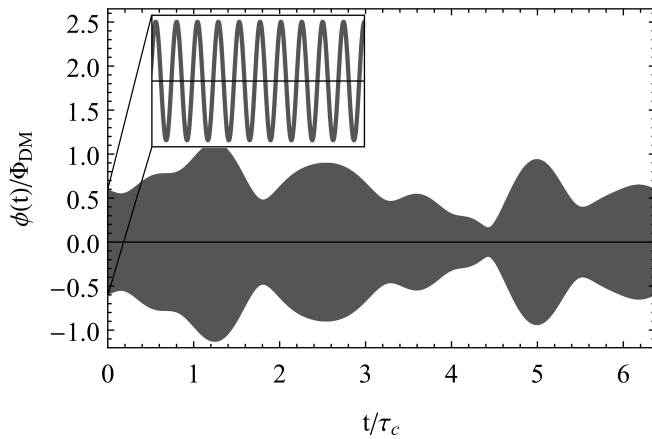


FIG. 1. Simulated VULF based on the approach in Ref. [41] with field value $\phi(t)$ and time normalized by Φ_{DM} and coherence time τ_c respectively. The inset plot displays the high-resolution coherent oscillation starting at $t = 0$.

lacking² and is becoming more relevant as experiments begin searching such regimes.

Here we focus on this regime, $T \ll \tau_c$, characteristic of experiments searching for ultralight (pseudo)scalars with masses $\lesssim 10^{-13}$ eV [33–39] that have field coherence times $\gtrsim 1$ day. This mass range is of significant interest as the lower limit on the mass of ultralight axions is down to 10^{-22} eV and can be further extended if it does not make up all of the DM [27]. Additionally, there has been recent theoretical motivation for “fuzzy dark matter” in the $10^{-22} - 10^{-21}$ eV range [27–30] and the so-called string “axiverse” extends down to 10^{-33} eV [31]. Similar arguments also apply to dilatons and moduli [32].

Figure 1 shows a simulated VULF field, illustrating the amplitude modulation present over several coherence times. At short time scales ($\ll \tau_c$) the field coherently oscillates at the Compton frequency, see the inset of Fig. 1, where the amplitude Φ_0 is fixed at a single value sampled from its distribution. An unlucky experimentalist could even have near-zero field amplitudes during the course of their measurement.

On these short time scales the DM signal $s(t)$ exhibits a harmonic signature,

$$s(t) = \gamma\xi\phi(t) \approx \gamma\xi\Phi_0 \cos(2\pi f_\phi t + \theta), \quad (1)$$

where γ is the coupling strength to a standard-model field and θ is an unknown phase. Details of the particular experiment are accounted for by the factor ξ . In this regime the amplitude Φ_0 is unknown and yields a time-averaged

energy density $\langle \phi(t)^2 \rangle_{T \ll \tau_c} = \Phi_0^2/2$. However, for times much longer than τ_c the energy density approaches the ensemble average determined by $\langle \Phi_0^2 \rangle = \Phi_{\text{DM}}^2$. This field oscillation amplitude is estimated by assuming that the average energy density in the bosonic field is equal to the local DM energy density $\rho_{\text{DM}} \approx 0.4 \text{ GeV/cm}^3$, and thus $\Phi_{\text{DM}} = \hbar(m_\phi c)^{-1} \sqrt{2\rho_{\text{DM}}}$.

The oscillation amplitude sampled at a particular time for a duration $\ll \tau_c$ is not simply Φ_{DM} , but rather a random variable whose sampling probability is described by a distribution characterizing the stochastic nature of the VULF. Until recently, most experimental searches have been in the $m_\phi \gg 10^{-13}$ eV regime with short coherence times $\tau_c \ll 1$ day. However, for smaller boson masses it becomes impractical to sample over many coherence times: for example, $\tau_c \gtrsim 1$ year for $m_\phi \lesssim 10^{-16}$ eV. Assuming that $\Phi_0 = \Phi_{\text{DM}}$ neglects the stochastic nature of the bosonic dark matter field [33–39].

The net field $\phi(t)$ is a sum of different field modes with random phases. The oscillation amplitude, Φ_0 , results from the interference of these randomly phased oscillating fields. This can be visualized as arising from a random walk in the complex plane, described by a Rayleigh distribution

$$p(\Phi_0) = \frac{2\Phi_0}{\Phi_{\text{DM}}^2} \exp\left(-\frac{\Phi_0^2}{\Phi_{\text{DM}}^2}\right), \quad (2)$$

analogous to that of chaotic (thermal) light [55]. This distribution implies that $\sim 63\%$ of all amplitude realizations will be below the r.m.s. value Φ_{DM} .

We refer to the conventional approach assuming $\Phi_0 = \Phi_{\text{DM}}$ as *deterministic* and approaches that account for the VULF amplitude fluctuations as *stochastic*. To compare these two approaches we choose a Bayesian framework and calculate the numerical factor affecting coupling constraints, allowing us to provide modified exclusion plots of previous deterministic constraints [33–39]. It is important to emphasize that different frameworks to interpret experimental data than presented here could change the magnitude of this numerical factor [56–59]. In any case, accounting for this stochastic nature will generically relax existing constraints as we show below.

Establishing constraints on coupling strength — We follow the Bayesian framework [60] (see application to VULFs in Ref. [41]) to determine constraints on the coupling strength parameter γ . Bayesian inference uses prior information (such as assuming that one candidate makes up all of the DM, or conditions imposed by the SHM) to derive posterior probability distributions for given propositions or model parameters. One additional prior we assume here is that the DM signal is well below the experimental noise floor. The central quantity of interest in our case is the posterior distribution for possible values

² We only found explicit investigation of the $T \ll \tau_c$ regime in Ref. [54] where the authors state the exponential distribution of the dark matter energy density, and by the authors of Ref. [53] discussing sensitivity in their Appendix E.

of γ , derived from Bayes theorem,

$$p(\gamma|D, f_\phi, \xi, I) = \mathcal{C} \int p(\Phi_0|I) d\Phi_0 \int p(\theta|I) d\theta \times \mathcal{L}(D|\gamma, \Phi_0, \theta, f_\phi, \xi, I). \quad (3)$$

The left-hand side of the equation is the posterior distribution for γ , where D represents the data, and the Compton frequency f_ϕ is a model parameter. \mathcal{C} is the normalization constant, and the likelihood $\mathcal{L}(\dots)$ is the probability of obtaining the data D given that the model and prior information I , such as those provided by the SHM, are true. In particular, we assume $p(\theta|I) = 1/(2\pi)$ is a uniform distribution and $p(\Phi_0|I)$ is the Rayleigh distribution shown in Eq. (2). The integrals on the right-hand side account for (to “marginalize over”) the unknown VULF phase θ and amplitude Φ_0 . Here we assumed that the prior distribution for possible γ , $p(\gamma, I)$, is sufficiently broad and uniform, ensuring that the derived posterior distribution is not affected. This assumed prior is consistent with previous work [33–39, 61].

It is important to note that “wind-type” experiments are sensitive to the relative velocity between the laboratory and the VULF. The projection of this velocity onto the sensitive axis of the experiment contains the assumed random component of the VULF. This random component increases the uncertainty of the derived coupling strength for a given measurement and needs to be taken into account. These experiments also utilize the daily modulation of this projection, due to the Earth’s rotation, to search for signals with an oscillation period much longer than the measurement time $T \ll 1/f_\phi$. The unknown initial phase θ of the VULF sets the amplitude of this daily oscillation and also needs to be marginalized. We describe how we account for velocity and daily modulation in the relevant experiments [33–36] in the Supplementary Material and focus solely on amplitude, Φ_0 , here.

If the posterior distribution, $p(\gamma|D, f_\phi, I)$, exhibits no evidence for a DM signal (no sharp peak) one can set constraints on the coupling strength γ . Such a constraint at the commonly employed 95% confidence level (CL), $\gamma_{95\%}$, is given by

$$2 \int_0^{\gamma_{95\%}} p(\gamma|D, f_\phi, \xi, I) d\gamma = 0.95. \quad (4)$$

Note that the factor of two comes from the normalization of the derived posterior distributions, Eqs. (5) and (6), since the coupling strength is allowed to be negative.

The posteriors in both the deterministic and stochastic treatments are derived in the Supplementary Material. In short, the two posteriors differ due to the additional marginalization over Φ_0 for the stochastic case, seen in the first integral of Eq. (3). Assuming white noise of variance σ^2 and a VULF DM signal well below the noise

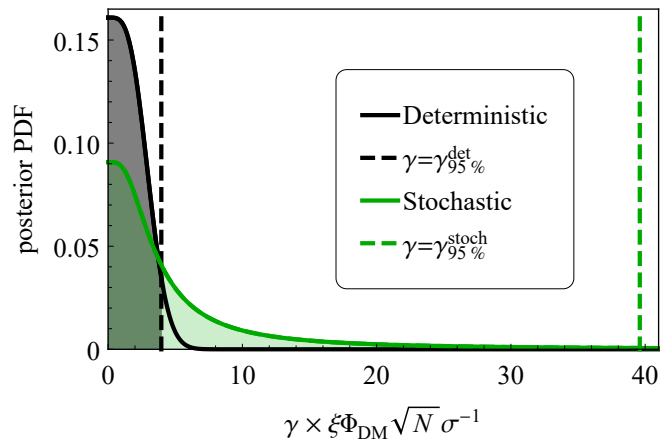


FIG. 2. Posterior distributions for the coupling strength γ in the deterministic and stochastic treatments, Eqs. (5) and (6) respectively. Due to the Lorentzian-like shape of the stochastic posterior one can clearly see the 95% limit is significantly larger $\gamma_{95\%}^{\text{stoch}}/\gamma_{95\%}^{\text{det}} = 9.98$. For the case of 90% confidence level the ratio is $\gamma_{90\%}^{\text{stoch}}/\gamma_{90\%}^{\text{det}} = 5.73$.

floor (current experimental regime), the posteriors are

$$p_{\text{det}}(x) = \mathcal{A} \exp(-x^2/4) I_0(x), \quad (5)$$

$$p_{\text{stoch}}(x) = \frac{\mathcal{B}}{1+x^2/4} \exp\left(-\frac{1}{1+x^2/4}\right). \quad (6)$$

Here $x \equiv \gamma \times \xi \Phi_{\text{DM}} \sqrt{N} \sigma^{-1}$, $I_0(x)$ is the modified Bessel function of the first kind, and $\mathcal{A} \approx 0.161$ and $\mathcal{B} \approx 0.247$ are the normalization constants. The derivation relies on the discrete Fourier transform for a uniform sampling grid of N points. The assumptions of the uniform grid and white noise can be relaxed, as shown in the Supplementary Material. The resulting normalized posteriors are shown in Fig. 2.

Examination of Eqs. (5), (6) and Fig. 2 reveals that the Lorentzian-like stochastic posterior is much broader than the Gaussian-like deterministic posterior. It is clear that for the fat-tailed stochastic posterior, the integration must extend considerably further into the tail, leading to larger values of $\gamma_{95\%}$ and thereby to weaker constraints, $\gamma_{95\%}^{\text{stoch}} > \gamma_{95\%}^{\text{det}}$. Explicit evaluation of Eq. (4) with the derived posteriors results in a relation between the constraints

$$\gamma_{95\%}^{\text{stoch}} \approx 10 \gamma_{95\%}^{\text{det}}, \quad (7)$$

where the numerical value of the scaling factor depends on CL, e.g. a 90% CL yields 5.73.

These results have been crosschecked via two alternative approaches. First, avoiding the use of the discrete Fourier transform, we derived approximate time-domain posteriors that hold for colored noise instruments and non-uniform sampling. This approximate approach yields a result consistent with Eq. (7). Additionally, results from a Monte Carlo (MC) approach using the pack-

age blueice [62] to model CASPER-ZULF [34] also indicate a significant effect. Details of these alternative approaches can be found in the Supplementary Material. We note that the value of the corrective factor may depend on the specific analysis and assumptions therein. Regardless of the chosen framework, this implies that existing constraints based on the deterministic model are overestimated by roughly one order of magnitude.

Revised exclusion plots – Ultralight DM candidates are theoretically well motivated and an increasing number of experiments are searching for them. Most of the experiments with published constraints thus far are haloscopes, sensitive to the local galactic DM and affected by Eq. (7). However, experiments that measure axions generated from a source, helioscopes or new-force searches, for example, do not fall under the assumptions made here. We illustrate how the existing constraints have been affected in Fig. 3 and provide more detailed exclusion plots for the axion-nucleon coupling g_{aNN} [33–35, 61] in Fig. 4 and for dilaton couplings [37–39] in Fig. 5.

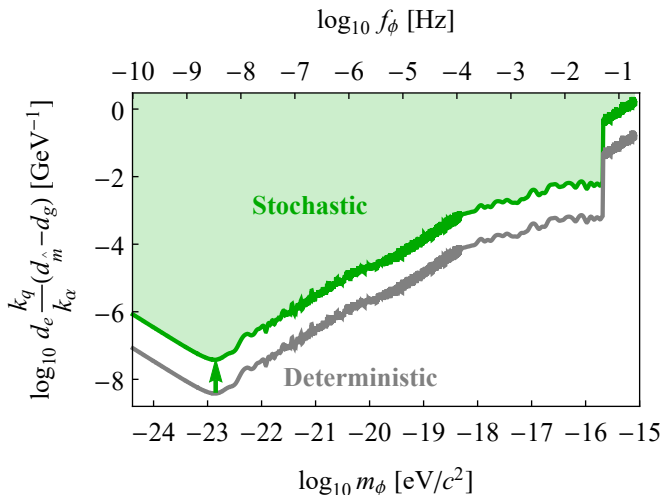


FIG. 3. The modified constraint, green line, based on the stochastic approach compared to previous laboratory constraints, gray line, based on the deterministic approach for the dilaton coupling strength d_e [37–39].

The published limits of CASPER-ZULF-Sidebands used a 90% CL, so we adjusted these data to a 95% CL for consistency using the factor determined from the ratio $\gamma_{95\%}^{\text{stoch}}/\gamma_{90\%}^{\text{det}}$. In addition, the combined corrections for the “wind-type” experiments CASPER-ZULF-Comagnetometer, -Sidebands, and nEDM include amplitude, velocity, and initial phase when appropriate (when $T \ll \tau_c$ and additionally $T \ll 1/f_\phi$ for phase). We adopt a straightforward MC approach to estimate the combined effect of these parameters, similar to that implemented in [34], yielding constraints a factor of ≈ 18 weaker than those derived assuming the deterministic parameters. The nEDM and CASPER-ZULF-Comagnetometer data were corrected by this factor, while the CASPER-

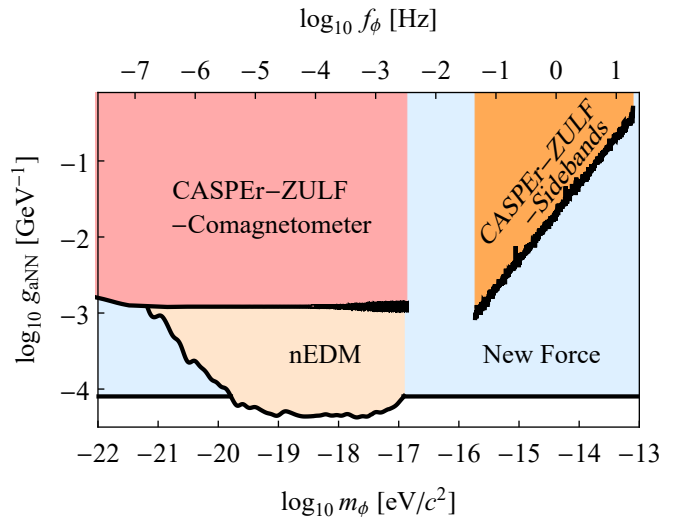


FIG. 4. An updated VULF exclusion plot of laboratory constraints for the axion-nucleon coupling, g_{aNN} , from the following experiments: CASPER-ZULF [34, 35], nEDM [33], and a new-force search using a K- ^3He comagnetometer [61].

ZULF-Sidebands data already took these parameters into account [34]. Details of these corrections can be found in the Supplementary Material, where different approaches are also discussed.

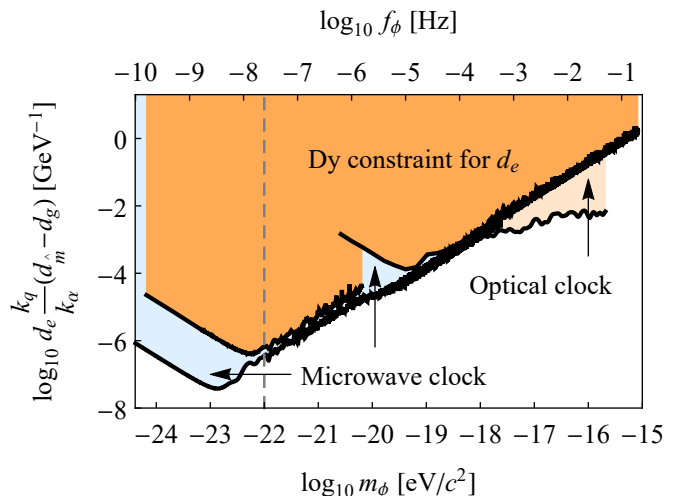


FIG. 5. An updated VULF exclusion plot of laboratory constraints for dilaton coupling strength d_e and linear combination (seen on y-axis). Details on the data for the dual rubidium and cesium cold atom fountain FO2 at LNE-SYRTE can be found in [38], for the two isotope dysprosium spectroscopy in [37], and from the global network of optical atomic clocks in [39]. The gray dashed line, $m_\phi \lesssim 10^{-22}$ eV, indicates where the assumption that m_ϕ makes up all the dark matter should be relaxed [27].

Conclusion – To interpret the results of an experiment searching for bosonic DM in the regime of measurement times smaller than the coherence time, stochastic

properties of the net field must be taken into account. An accurate description accounts for the Rayleigh distributed amplitude Φ_0 , where the variation is induced by the random phases of individual virialized fields. The Bayesian framework adopted to account for this stochastic nature yields a correction of about one order of magnitude, relaxing seven existing bosonic DM constraints in this regime. In the event of a bosonic DM discovery, the stochastic properties of the field would result in large uncertainty in the determination of coupling strength or local average energy density in this regime.

Data Availability – All conclusions made in this paper can be reproduced using the information presented in the manuscript and/or Supplementary Material. Additional information is available upon reasonable request to the corresponding author. For access to the experimental data presented here please contact the corresponding authors of the respective papers.

Acknowledgments – We thank Eric Adelberger and William A. Terrano for pointing out the need to account for the unknown phase in the CASPER-ZULF Comagnetometer analysis. We thank Kent Irwin, Marina Gil Sendra, and Martin Engler for helpful discussions and suggestions. We thank M. Zawada, N. A. Leefler, and A. Hees for providing raw data for the published deterministic constraints. We also thank Jelle Aalbers for helpful discussions and expert advice on the blueice inference framework. Jan Conrad appreciates the support by the Knut and Alice Wallenberg Foundation. This project has received funding from the European Research Council (ERC) under the European Unions Horizon 2020 research and innovation programme (grant agreement No 695405). We acknowledge the partial support of the U.S. National Science Foundation, the Simons and Heising-Simons Foundations, and the DFG Reinhart Koselleck project.

-
- [1] S. Dimopoulos and G. F. Giudice, *Physics Letters B* **379**, 105 (1996).
- [2] N. Arkani-Hamed, L. Hall, D. Smith, and N. Weiner, *Phys. Rev. D* **62**, 105002 (2000).
- [3] T. R. Taylor and G. Veneziano, *Physics Letters B* **213**, 450 (1988).
- [4] T. Damour and A. M. Polyakov, *Nuclear Physics B* **423**, 532 (1994).
- [5] R. D. Peccei and H. R. Quinn, *Physical Review D* (1977), 10.1103/PhysRevD.16.1791.
- [6] R. D. Peccei and H. R. Quinn, *Physical Review Letters* (1977), 10.1103/PhysRevLett.38.1440.
- [7] S. Weinberg, *Physical Review Letters* **40**, 223 (1978).
- [8] F. Wilczek, *Physical Review Letters* **40**, 279 (1978).
- [9] J. E. Kim, *Physical Review Letters* **43**, 103 (1979).
- [10] P. W. Graham, I. G. Irastorza, S. K. Lamoreaux, A. Lindner, and K. A. van Bibber, *Annual Review of Nuclear and Particle Science* **65**, 485 (2015), arXiv:1602.00039v1.
- [11] I. G. Irastorza and J. Redondo, *Progress in Particle and Nuclear Physics* **102**, 89 (2018).
- [12] S. DePanfilis, A. C. Melissinos, B. E. Moskowitz, J. T. Rogers, Y. K. Semertzidis, W. U. Wuensch, H. J. Halama, A. G. Prodell, W. B. Fowler, and F. A. Nezrick, *Physical Review Letters* **59**, 839 (1987).
- [13] W. U. Wuensch, S. De Panfilis-Wuensch, Y. K. Semertzidis, J. T. Rogers, A. C. Melissinos, H. J. Halama, B. E. Moskowitz, A. G. Prodell, W. B. Fowler, and F. A. Nezrick, *Physical Review D* **40**, 3153 (1989).
- [14] C. Hagmann, P. Sikivie, N. S. Sullivan, and D. B. Tanner, *Physical Review D* (1990), 10.1103/PhysRevD.42.1297.
- [15] S. J. Asztalos, G. Carosi, C. Hagmann, D. Kinion, K. van Bibber, M. Hotz, L. J. Rosenberg, G. Rybka, J. Hoskins, J. Hwang, P. Sikivie, D. B. Tanner, R. Bradley, and J. Clarke, *Physical Review Letters* **104**, 041301 (2010).
- [16] P. W. Graham and S. Rajendran, *Physical Review D - Particles, Fields, Gravitation and Cosmology* **88**, 1 (2013), arXiv:arXiv:1306.6088v2.
- [17] D. Budker, P. W. Graham, M. Ledbetter, S. Rajendran, and A. O. Sushkov, *Physical Review X* **4**, 021030 (2014), arXiv:1306.6089.
- [18] B. M. Brubaker, L. Zhong, S. K. Lamoreaux, K. W. Lehnert, and K. A. van Bibber, *Physical Review D* **96**, 123008 (2017).
- [19] A. Caldwell, G. Dvali, B. Majorovits, A. Millar, G. Raffelt, J. Redondo, O. Reimann, F. Simon, and F. Steffen, *Physical Review Letters* **118**, 091801 (2017).
- [20] M. C. Miller, *Nature* **551**, 36 (2017).
- [21] W. Chung, in *Proceedings of Science* (2015).
- [22] J. Choi, H. Themann, M. J. Lee, B. R. Ko, and Y. K. Semertzidis, *Physical Review D* **96**, 061102 (2017).
- [23] B. T. McAllister, G. Flower, E. N. Ivanov, M. Goryachev, J. Bourhill, and M. E. Tobar, *Physics of the Dark Universe* **18**, 67 (2017).
- [24] D. Alesini, D. Babusci, D. Di Gioacchino, C. Gatti, G. Lamanna, and C. Ligi, (2017), arXiv:1707.06010.
- [25] Y. V. Stadnik and V. V. Flambaum, *Physical Review Letters* **114**, 161301 (2015).
- [26] H. Grote and Y. V. Stadnik, “Novel signatures of dark matter in laser-interferometric gravitational-wave detectors,” (2019), arXiv:1906.06193.
- [27] D. J. Marsh, *Physics Reports* **643**, 1 (2016), arXiv:0610440 [astro-ph].
- [28] D. J. Marsh and J. Silk, *Monthly Notices of the Royal Astronomical Society* (2014), 10.1093/mnras/stt2079.
- [29] W. Hu, R. Barkana, and A. Gruzinov, *Physical Review Letters* **85**, 1158 (2000).
- [30] L. Hui, J. P. Ostriker, S. Tremaine, and E. Witten, *Physical Review D* (2017), 10.1103/PhysRevD.95.043541, arXiv:1610.08297.
- [31] A. Arvanitaki, S. Dimopoulos, S. Dubovsky, N. Kaloper, and J. March-Russell, *Physical Review D* **81**, 123530 (2010).
- [32] A. Arvanitaki, J. Huang, and K. Van Tilburg, *Phys. Rev. D* **91**, 015015 (2015).
- [33] C. Abel, N. J. Ayres, G. Ban, G. Bison, K. Bodek, V. Bondar, M. Daum, M. Fairbairn, V. V. Flambaum, P. Geltenbort, *et al.*, *Physical Review X* **7**, 041034 (2017).
- [34] A. Garcon, J. W. Blanchard, G. P. Centers, N. L. Figueroa, P. W. Graham, D. F. Jackson Kimball, S. Rajendran, A. O. Sushkov, Y. V. Stadnik, A. Wickenbrock, T. Wu, and D. Budker, *Science Advances* **5**, eaax4539

- (2019), arXiv:1902.04644.
- [35] T. Wu, J. W. Blanchard, G. P. Centers, N. L. Figueroa, A. Garcon, P. W. Graham, D. F. J. Kimball, S. Rajendran, Y. V. Stadnik, A. O. Sushkov, A. Wickenbrock, and D. Budker, *Physical Review Letters* **122**, 191302 (2019), arXiv:1901.10843.
- [36] W. A. Terrano, E. G. Adelberger, C. A. Hagedorn, and B. R. Heckel, *Physical Review Letters* **122**, 231301 (2019), arXiv:1902.04246.
- [37] K. Van Tilburg, N. Leefler, L. Bougas, and D. Budker, *Physical Review Letters* **115**, 011802 (2015).
- [38] A. Hees, J. Guéna, M. Abgrall, S. Bize, and P. Wolf, *Physical Review Letters* **117**, 061301 (2016).
- [39] P. Wcisło, P. Ablewski, K. Beloy, S. Bilicki, M. Bober, R. Brown, R. Fasano, R. Ciuryło, H. Hachisu, T. Ido, J. Lodewyck, A. Ludlow, W. McGrew, P. Morzyński, D. Nicolodi, M. Schioppo, M. Sekido, R. Le Targat, P. Wolf, X. Zhang, B. Zjawin, and M. Zawada, *Science Advances* **4**, eaau4869 (2018).
- [40] A. A. Geraci and A. Derevianko, *Phys. Rev. Lett.* **117**, 261301 (2016).
- [41] A. Derevianko, *Phys. Rev. A* **97**, 042506 (2018), arXiv:1605.09717.
- [42] A. Derevianko, *Physical Review A* **97**, 042506 (2018), arXiv:1605.09717.
- [43] F. Zwicky, Published in *Helvetica Physica Acta* (1933), 10.1007/s10714-008-0707-4, arXiv:1711.01693.
- [44] M. Kuhlen, A. Pillepich, J. Guedes, and P. Madau, *The Astrophysical Journal* **784**, 161 (2014).
- [45] K. Freese, M. Lisanti, and C. Savage, *Reviews of Modern Physics* **85**, 1561 (2013), arXiv:1209.3339.
- [46] J. Diemand, M. Kuhlen, P. Madau, M. Zemp, B. Moore, D. Potter, and J. Stadel, *Nature* **454**, 735 (2008).
- [47] P. Sikivie and Q. Yang, *Physical Review Letters* **103**, 111301 (2009), arXiv:0901.1106.
- [48] S. Davidson, *Astroparticle Physics* (2015), 10.1016/j.astropartphys.2014.12.007.
- [49] J. Berges and J. Jaeckel, *Physical Review D - Particles, Fields, Gravitation and Cosmology* (2015), 10.1103/PhysRevD.91.025020.
- [50] D. F. Jackson Kimball, D. Budker, J. Eby, M. Pospelov, S. Pustelny, T. Scholtes, Y. V. Stadnik, A. Weis, and A. Wickenbrock, *Physical Review D* (2018), 10.1103/PhysRevD.97.043002.
- [51] M. Y. Khlopov, B. A. Malomed, and Y. B. Zeldovich, *Monthly Notices of the Royal Astronomical Society* **215**, 575 (1985).
- [52] J. D. Romano and N. J. Cornish, *Living Reviews in Relativity* **20**, 1 (2017), arXiv:1608.06889.
- [53] J. W. Foster, N. L. Rodd, and B. R. Safdi, *Physical Review D* **97**, 123006 (2018).
- [54] S. Knirck, A. J. Millar, C. A. O’Hare, J. Redondo, and F. D. Steffen, *Journal of Cosmology and Astroparticle Physics* **2018**, 051 (2018), arXiv:1806.05927.
- [55] R. Loudon, *The Quantum Theory of Light*, 2nd ed. (Oxford University Press, 1983).
- [56] R. Protassov, D. A. van Dyk, A. Connors, V. L. Kashyap, and A. Siemiginowska, *The Astrophysical Journal* **571**, 545 (2002).
- [57] G. Cowan, K. Cranmer, E. Gross, and O. Vitells, *The European Physical Journal C* **71**, 1 (2011).
- [58] J. Conrad, “Statistical issues in astrophysical searches for particle dark matter,” (2015).
- [59] M. Tanabashi, K. Hagiwara, K. Hikasa, K. Nakamura, Y. Sumino, F. Takahashi, J. Tanaka, K. Agashe, G. Aielli, C. AMSler, *et al.*, “Review of Particle Physics,” (2018), arXiv:0601168 [astro-ph].
- [60] P. Gregory, *Bayesian Logical Data Analysis for the Physical Sciences: A Comparative Approach with Mathematica Support* (Cambridge University Press, 2010).
- [61] G. Vasilakis, J. M. Brown, T. W. Kornack, and M. V. Romalis, *Physical Review Letters* **103**, 261801 (2009).
- [62] J. Aalbers, K. Dundas Morâ, and B. Pelssers, “JelleAalbers/blueice: v1.0.0-beta.2,” (2019).

Supplementary material

I. CALCULATING THE EXCLUSION PLOT REVISION FACTOR

We would like to point the reader toward a number of resources, Refs. [1–5], illustrating the sensitivity of the exclusion limit to the chosen analysis method. We discuss the methods presented in the paper below where varying results could be due to the chosen analysis. It is important to emphasize that, regardless of the chosen analysis, accounting for the stochastic behavior generically relaxes constraints that did not.

A. Setup

The ultralight dark matter fields are composed of a large number of individual modes with randomized phases. As such, due to the central-limit theorem, the VULF fields belong to a broad class of Gaussian random fields that are encountered in many subfields of physics. The statistical properties of such fields are fully described by the two-point correlation functions in the time domain or power-spectral densities in frequency space, see VULF-specific discussion in Ref. [6].

Here we consider an ultralight dark matter search in the regime when the observation time T is shorter than the coherence time τ_c of dark matter field. Because on these short time scales the VULF oscillations are nearly coherent, these data streams can be fit to an oscillatory function

$$s(t) = \gamma \xi \phi(t) = \gamma \xi \Phi_0 \cos(2\pi f_\phi t + \theta). \quad (1)$$

Here f_ϕ is the field Compton frequency (specific to a particular realization of the VULF as the frequency is Doppler shifted by the relative motion with respect to the detector), θ is an unknown yet fixed phase, ξ is a constant determined by the details of the experiment, and γ is a coupling strength that is, assuming a null result, to be constrained by the measurement. We fix the amplitude of the DM field to be positive, $\Phi_0 \geq 0$ and the phase θ of the field to lie in the range $[0 - 2\pi)$. The coupling strength γ can have an arbitrary sign.

In the conventional approach the DM field amplitude Φ_0 is fixed to its root-mean-square value Φ_{DM} , defined in the main body of the paper. We refer to such an approach as *deterministic*. The key issue is that for a given experimental run $T \ll \tau_c$, the value of the VULF amplitude Φ_0 can substantially differ from Φ_{DM} ; the VULF amplitude randomly fluctuates. This is apparent from the simulation presented in Fig. 1 of the main text. Thus Φ_0 has to be treated as a marginalization parameter in the analysis. We refer to this treatment as *stochastic*. This has important implications for establishing constraints on γ .

The probability densities for the DM field amplitude in the two approaches can be summarized as

$$p(\Phi_0|\Phi_{\text{DM}}) = \begin{cases} \delta(\Phi_0 - \Phi_{\text{DM}}), & \text{deterministic} \\ \frac{2\Phi_0}{\Phi_{\text{DM}}^2} \exp\left(-\frac{\Phi_0^2}{\Phi_{\text{DM}}^2}\right), & \text{stochastic} \end{cases} \quad (2)$$

The stochastic probability distribution for the amplitude can be recast into probability distribution for the local energy density $\rho = \Phi_0^2 f_c^2 / 2$ of the dark matter field,

$$p(\rho|\rho_{\text{DM}})d\rho = \frac{1}{\rho_{\text{DM}}} e^{-\rho/\rho_{\text{DM}}} d\rho, \quad (3)$$

in agreement with Ref. [7].

Below, we show that for a fixed value of $\Phi_0 = \Phi_{\text{DM}}$ the posterior distribution for γ is Gaussian-like, dropping exponentially for large values of γ . Then, we allow Φ_0 to be a random variable with a probability distribution dictated by the standard halo model. In this stochastic treatment, we show that the poster distribution for γ is Lorentzian-like, with a long $1/\gamma^2$ tail.

The shape of the posterior distribution $p(\gamma)$ has immediate implications for placing constraints, and also in the event of a DM detection, as the stochastic nature of the VULF affects uncertainty in the value of γ . Here, we assume that the dark matter signal is well below the detection threshold, an assumption consistent with current experimental results. Then the most likely value of γ is zero and a constraint at the 95% confidence level, $\gamma_{95\%}$, can be determined from

$$2 \int_0^{\gamma_{95\%}} p(\gamma) d\gamma = 0.95. \quad (4)$$

Since the limits on γ are derived by integrating the posterior distribution, the integration must proceed to larger values of γ for the fat-tailed distribution. This leads to substantially different 95% C.L. limits on γ in the two treatments.

In the following, we derive the coupling-strength posteriors using different methods: discrete Fourier transform, time-domain analysis, calculate the scaling factor using a Monte Carlo (MC) approach with blueice [8], and a signal model comparison using another MC method.

B. Derivation of coupling-strength posteriors using the discrete Fourier transform

As an analytically treatable case, we assume that the data stream was acquired on a uniform time grid. Considering the oscillating nature of the signal (1), we will work in frequency space, applying discrete Fourier transform (DFT) to the data. The data set is assumed to include N measurements, taken over the total observation time T . To make the derivation as transparent as possible, we assume that the intrinsic instrument noise is white with variance σ^2 . The assumption of white noise, however, is hardly necessary, and the derivation remains valid for the more general case of colored noise. The generalization can be accomplished by replacing $N\sigma^2$ with the noise power spectral density $\tilde{S}(f_p)$, where f_p is the DFT frequency. We use DFT notation and definitions of Ref. [6] (see appendix of that paper for a review of Bayesian statistics in frequency space).

Suppose we would like to establish constraints on the coupling strength γ at one of the DFT frequencies $f_p = f_c$. If \tilde{d}_p is the DFT amplitude of the original data, the likelihood at f_p is given by

$$\mathcal{L}(\tilde{d}_p|\Phi_0, \gamma, \phi) = \frac{1}{\pi N\sigma^2} \exp\left\{-\frac{|\tilde{d}_p - \tilde{s}_p|^2}{N\sigma^2}\right\}, \quad (5)$$

where $\tilde{s}_p = N\gamma\xi\Phi_0 e^{i\theta}/2$ is the DFT amplitude of the signal (1). Marginalizing over phase θ with a uniform prior [see Eq.(3) of the main text], we arrive at the phaseless likelihood

$$\mathcal{L}(\tilde{d}_p|\Phi_0, \gamma) = \frac{1}{\pi N\sigma^2} e^{-\frac{|\tilde{d}_p|^2}{N\sigma^2}} \exp\left(-\frac{N\gamma^2\xi^2\Phi_0^2}{4\sigma^2}\right) I_0\left(\frac{\gamma\xi\Phi_0|\tilde{d}_p|}{\sigma^2}\right), \quad (6)$$

where I_0 is the modified Bessel function of the first kind. This type of Rice-like distribution has been derived earlier, see, e.g., Eq. (10) of Ref. [9].

According to the Bayes theorem, the posterior distribution $p(\gamma|\tilde{d}_p, \Phi_0)$ for coupling strength γ is proportional to the likelihood $\mathcal{L}(\tilde{d}_p|\Phi_0, \gamma)$,

$$p(\gamma|\tilde{d}_p, \Phi_0) = \mathcal{C} \exp\left(-\frac{N\gamma^2\xi^2\Phi_0^2}{4\sigma^2}\right) I_0\left(\frac{\gamma\xi\Phi_0|\tilde{d}_p|}{\sigma^2}\right), \quad (7)$$

with \mathcal{C} being the normalization constant [10]. This means that, given the data, we can explicitly construct probability distribution for the coupling strength γ . Since we are focusing on establishing constraints, we will assume that the DM signal is well below the detection threshold and we fix $|\tilde{d}_p|^2$ at its average value of $N\sigma^2$,

$$p(\gamma|\Phi_0) = \mathcal{C} \exp\left(-\frac{N\gamma^2\Phi_0^2}{4\sigma^2}\right) I_0\left(\frac{\sqrt{N}\gamma\xi\Phi_0}{\sigma}\right). \quad (8)$$

The posterior depends on the assumed value of DM field amplitude Φ_0 . In the deterministic treatment, $\Phi_0 \equiv \Phi_{\text{DM}}$, thus $p_{\text{det}}(\gamma) = p(\gamma|\Phi_0 \equiv \Phi_{\text{DM}})$. This leads to the ‘‘deterministic’’ posterior

$$p_{\text{det}}(\gamma) = \mathcal{C} \exp\left(-\frac{N\gamma^2\xi^2\Phi_{\text{DM}}^2}{4\sigma^2}\right) I_0\left(\frac{\sqrt{N}\gamma\xi\Phi_{\text{DM}}}{\sigma}\right), \quad (9)$$

shown in Fig. 2 of the main text. Numerical integration, Eq. (4), of the posterior yields the 95% C.L. constraint

$$\gamma_{95\%}^{\text{det}} \approx 3.95 \frac{\sigma}{\sqrt{N}} \Phi_{\text{DM}}^{-1}. \quad (10)$$

As we show below, this ‘‘deterministic’’ constraint is off by an order of magnitude.

Now we take into account that the field amplitude Φ_0 for a given experimental run is uncertain. This can be done formally by marginalizing over the field amplitudes with the Rayleigh distribution,

$$p_{\text{stoch}}(\gamma) = \int_0^\infty p(\Phi_0|\Phi_{\text{DM}})p(\gamma|\Phi_0)d\Phi_0.$$

The result is

$$p_{\text{stoch}}(\gamma) = \frac{\mathcal{C}'}{1 + \gamma^2 \xi^2 \Phi_{\text{DM}}^2 N / (4\sigma^2)} \exp\left(-\frac{1}{1 + \gamma^2 \xi^2 \Phi_{\text{DM}}^2 N / (4\sigma^2)}\right), \quad (11)$$

where \mathcal{C}' is a normalization constant. Again we fixed $|\tilde{d}_p|^2$ at its average value of $N\sigma^2$.

Below we will also give an alternative derivation of this posterior using the two-point correlation function for VULFs that avoids introduction of the Rayleigh distribution.

A comparison of the two resulting posteriors in deterministic and stochastic approaches is given in Fig. 2 of the main text. It is apparent that the stochastic distribution is wider. While the deterministic posterior is Gaussian-like, the stochastic posterior exhibits a Lorentzian-like character.

Now with the posterior distribution in hand, we use Eq. (4) to derive the 95% C.L. constraint

$$\gamma_{95\%}^{\text{stoch}} \approx 39.4 \frac{\sigma}{\sqrt{N}} \Phi_{\text{DM}}^{-1}. \quad (12)$$

Comparing this result with Eq. (10) derived in the deterministic treatment, we find

$$\gamma_{95\%}^{\text{stoch}} \approx 10 \gamma_{95\%}^{\text{det}}. \quad (13)$$

The exact value of the scaling factor depends on the confidence level. In any case, the stochastic constraint is always weaker than the deterministic one due to the stochastic distribution being fat-tailed, decaying only as γ^{-2} for large γ . The relation (13) immediately implies that the constraints derived in the “deterministic” approach are overestimated by an order of magnitude. This conclusion does not depend on the assumed white noise model, as in all the formulas one can simply replace $N\sigma^2$ with the power spectral density $\tilde{S}(f_p)$ for a specific measurement apparatus. This replacement does not modify the relation (13) between the stochastic and deterministic constraints.

Finally, we re-derive the stochastic posterior (11) starting directly from the stochastic likelihood in the frequency space. This approach avoids explicit introduction of the Rayleigh distribution of the field amplitude. The relevant likelihood at DFT frequency f_p is given by (see, e.g., [6])

$$\mathcal{L}_{\text{stoch}}(\tilde{d}_p|\gamma) = \frac{1}{\pi \Sigma_p} e^{-\frac{|\tilde{d}_p|^2}{\Sigma_p}}, \quad (14)$$

with Σ_p being a combined power spectral density of the device noise $N\sigma^2$ and DM signal $\gamma^2 \xi^2 \langle |\tilde{\phi}_p|^2 \rangle$.

We compute $\tilde{g}_p = \langle |\tilde{\phi}_p|^2 \rangle$ using the Wiener-Khinchin theorem. To this end we require the DM field auto-correlation function $g(\tau) = \langle \phi(t)\phi(t+\tau) \rangle$. This function was computed in Ref. [6] using SHM priors. In the relevant limit of $\tau \ll \tau_c$ it reads

$$g(\tau) = \frac{1}{2} \Phi_{\text{DM}}^2 \cos(2\pi f_c \tau), \quad (15)$$

corresponding to a coherent oscillation at the Compton frequency. There is an important subtlety in applying the Wiener-Khinchin theorem in the limit of $T \ll \tau_c$, as this theorem is usually stated in the opposite limit. The exact relation between the power spectral density and the auto-covariance functions in DFT reads (see, e.g., Ref. [6])

$$\tilde{g}_p = N g(0) + 2 \sum_{l=1}^{N-1} (N-l) g\left(\frac{T}{N} l\right) \cos\left(\frac{2\pi}{N} p l\right), \quad (16)$$

leading to the PSD at the target Compton frequency ($N \gg 1$),

$$\tilde{g}_p = \Phi_{\text{DM}}^2 \frac{N^2}{4}. \quad (17)$$

Returning to the likelihood of the stochastic signal (14), the combined PSD reads,

$$\Sigma_p = N\sigma^2 + \gamma^2 \tilde{g}_p = N\sigma^2 + \gamma^2 \xi^2 \Phi_{\text{DM}}^2 \frac{N^2}{4}.$$

Plugging Σ_p into the stochastic likelihood (14) and using the Bayes theorem immediately yields the stochastic posterior (11). Notice that the Lorentzian-like shape of the stochastic posterior is entirely due to the normalization pre-factor in the Gaussian likelihood (14).

C. Approximate time-domain analysis

The results above can be also obtained in approximate way, without alluding to the DFT. Indeed, in time domain the Gaussian likelihood reads

$$\mathcal{L} \propto \exp\left(-\frac{1}{2}(\mathbf{d} - \mathbf{s})^T E^{-1}(\mathbf{d} - \mathbf{s})\right), \quad (18)$$

where E is the covariance matrix for the intrinsic noise of the instrument. For a white noise of variance σ^2 , $E_{ij} = \delta_{ij}\sigma^2$. Further, \mathbf{d} and \mathbf{s} are data and DM signal vectors composed of elements $d(t_i)$ and $s(t_i)$ on the time grid $\{t_i\}$. This likelihood simply states that the residuals are consistent with the instrument noise. The Gaussian likelihood is the starting point for developing many practically used data analysis techniques, such as the periodogram and matched filter techniques.

We demonstrate a similar result to Eq. (13) by taking the large limit of γ in the likelihood (18). First, we marginalize over the phase θ arriving at

$$\int p(\theta|I)\mathcal{L}d\theta \sim \exp\left(-\frac{x^2}{4}\frac{\Phi_0^2}{\Phi_{\text{DM}}^2}\right).$$

Here we took into account that $\sum_{i=1}^N \cos^2(2\pi f_\phi t_i + \theta) = N/2$ when averaged over θ . For the stochastic case we additionally integrate the above equation over Φ_0 with amplitude distribution (2) leading to $p_{\text{det}}(x) \propto \exp(-x^2/4)$ and $p_{\text{stoch}}(x) \propto \frac{1}{1+x^2/4}$. As in the main text $x \equiv \gamma \times \xi \Phi_{\text{DM}} \sqrt{N} \sigma^{-1}$. These formulas recover the tail behavior of the rigorous DFT results (9,11) and support our claim that in the stochastic treatment, the posterior assumes Lorentzian-like shape slowly decaying as γ^{-2} . Using these approximate posteriors we compute the ratio of $\gamma_{95\%}$ constraints to be ≈ 9.2 consistent with the more rigorous Eq. (13). Moreover, this result holds for the most general case of colored noise and non-uniform time grids, as in this case $x = \gamma \xi \Phi_{\text{DM}} \times \left[\sum_{i,j=1}^N (E^{-1})_{ij} \cos(2\pi f_\phi(t_i - t_j))\right]^{1/2}$; this modification does not affect the derived ratio between the widths of the two distributions.

D. Blueice Monte Carlo

Here we use a method widely used in astroparticle physics [11] to compare to the Bayesian approach above. In the case encountered here, we find that Wilks theorem does not hold since the test statistic distribution of many MC simulated datasets does not follow a χ^2 -distribution. The reason for this is in part due to the fact that we are not using the profile likelihood but marginalize over the amplitude fluctuation by drawing from the Rayleigh distribution in each MC realization. In a situation like this, one has to resort to doing a so-called Neyman construction, see e.g. discussion in Ref. [12].

The decisive feature of a Neyman construction is that it provides the statistically desired properties (in this case the coverage of the confidence intervals). It uses the distribution of the test statistic as estimated by many MC simulations instead of the asymptotic distribution used in Wilks theorem. For a given signal strength γ , the test statistic distribution is obtained by running many MC simulations at that signal strength. The critical value is the value of the test statistic at the 90th (or 95th) percentile of the distribution for a test at the 90% (or 95%) confidence level. This procedure is repeated for different signal strengths such that a critical value curve as a function of the signal strength is obtained. The upper limit on the signal strength for a given measurement (or MC simulation) is then given by the value at which the likelihood crosses the critical value curve.

The correction factor is finally not determined from a single experiment but rather from an ensemble of experiments over which the so called sensitivity (median limit in case of no signal) is calculated. The correction factor is then defined analogous to the case of the Bayesian analysis as:

$$\text{correction} = \frac{\text{median}(\mathbf{u}_{\text{stochastic}})}{\text{median}(\mathbf{u}_{\text{deterministic}})} \quad (19)$$

where \mathbf{u} is a large number of upper limits at a certain confidence level. Initial results from the simulations show a correction factor of 4.4 at the 95% confidence level when including only the amplitude distribution. We show an estimate of the correction including the remaining parameters in the next section.

E. Additional parameters

The gradient coupling of a bosonic field introduces an additional factor to the signal (1) proportional to $\vec{v} \cdot \vec{e}$ where \vec{v} is the DM velocity in the lab frame and \vec{e} is the sensitive axis of the experiment. The velocity, \vec{v} , can be written in terms of separate contributions with the leading term being the Sun's velocity toward Cygnus, additional modulation due to Earth's rotation (including orbit), and the random contribution of the field's velocity. We assume full modulation from the Earth's rotation, i.e the detector rotates parallel and perpendicular to the Cygnus component daily for a detector with sensitive axis $\hat{e} = \hat{z}$. These approximations give the expression $\vec{v} \cdot \vec{e} \approx v \cos(2\pi f_E t)$ where $f_E = 1/\text{day}$. We use a truncated (at the escape velocity) Gaussian distribution for the field velocity with mean value and spread of $10^{-3}c$, where we assume the Sun's speed is the same. This allows us to write a new definition of the signal as

$$s(t) = \gamma \xi \Phi_0 m_\phi \cos(2\pi f_\phi t + \theta) \vec{v} \cdot \vec{e} \approx \gamma \xi v \Phi_0 m_\phi \cos(2\pi f_\phi t + \theta) \cos(2\pi f_E t). \quad (20)$$

This expression naturally defines three regimes: writing down the coherent oscillation assumes we are in the middle regime of $T \ll \tau_c$ and the third regime occurs when the daily modulation dominates for $1/f_E < T \ll 1/f_\phi$. We use this model to calculate the correction in the $T < 1/f_\phi$ regime for the CASPER-ZULF-Comagnetometer data presented in Ref. [13].

In short, we compare MC signal amplitudes under the two signal assumptions (stochastic vs. deterministic parameters). To do so we generate 10^6 MC data for each frequency f_ϕ , choosing v , θ , and Φ_0 from their respective distributions, sampling for a total time T of 30 days at a rate above a Nyquist frequency set by f_E . The maximum Fourier amplitude is calculated for each data generating a distribution of power at the target f_ϕ frequency. The threshold amplitude A_t is calculated for each distribution such that 95% of the values are above A_t (this signal threshold guarantees detection at originally stated confidence). This value is compared to the deterministic data, generated by mirroring the assumptions made in the original paper [13], where the ratio between A_t and the deterministic power provides the correction factor to be applied to the original exclusion plot. We note that this MC approach is similar to the CL_s method [5], commonly used for upper limits in high energy particle physics, where we are calculating the ratio of two different signal CL_s exactly.

For the correction of frequencies above $1/T$ we compare the stochastic and deterministic signal models ignoring daily modulation and obtain a value of 18, analogous to the value calculated in Ref. [14] which simply uses the distributions of the parameters Φ_0 , v . We acknowledge the fact that the variation of the three parameters discussed here may be correlated, and that a more thorough theoretical treatment may provide some corrections. Nonetheless, the results presented here, by blueice, and in Ref. [14] support our argument that this variation should be considered when constructing exclusion plots in the appropriate regimes.

1. Constraints below frequency resolution ($1/T$)

In this section we discuss marginalization over the unknown phase θ of the VULF and, in particular, the effect of this marginalization on searches for VULFs with frequencies below $1/T$. This problem was the subject of a recent debate in the literature related to the CASPER-Wind-ZULF-Comagnetometer limits originally presented in Ref. [13]. The comment [15] on the published article [13] correctly pointed out that the limits for frequencies below the $1/T$ frequency resolution should not improve compared to limits for frequencies above the $1/T$ frequency resolution. This is true and the mistake in Ref. [13] came from not marginalizing over the uniform distribution of phase, θ in Eq. (20) above, and erroneously assuming the average signal amplitude in this limit $\propto \frac{1}{2\pi} \int |\sin(\theta)| d\theta = 2/\pi$, a deterministic approach to θ similar in principle to the erroneous deterministic approaches to $\sqrt{\text{VULF}}$ amplitudes and velocities [16]. However, after accounting for this unknown phase as discussed both in the present work and in the reply [16], the authors of the comment [15] still disagreed with the corrected limit published here.

The resolution of this debate is rooted in how constraints on couplings of VULF dark matter to standard model particles and fields should be interpreted. Even when assuming that VULF dark matter is well described by the SHM, at a particular time and place the experimentally observable signal is affected by a number of unknown VULF parameters beyond the coupling strength such as the phase, velocity, and amplitude. If the duration T of an experiment is too short to broadly sample the distribution of the unknown VULF parameters, then in actuality the experiment excludes the existence of VULF dark matter over some finite volume of a multi-dimensional space of the unknown parameters. To condense the results of a VULF dark matter search into a two-dimensional plot of coupling strength vs. frequency, it is necessary to marginalize over the other unknown VULF parameters. While the authors of the comment [15] object to this marginalization, arguing that for particular phases θ the constraints on couplings could be much weaker, in fact it is entirely reasonable to plot constraints on couplings ruled out over 95% of the multi-dimensional unknown VULF parameter space. Furthermore, as we note here, the authors of the comment [15] have

treated the amplitude and velocity of the VULF dark matter as deterministic in their own experiment [17]. For particular (but unlikely) VULF velocities and amplitudes, the experiment [17] is insensitive to VULF couplings. In order to constrain VULF dark matter couplings in the regime where T is shorter than either the coherence time or period of the VULF, it is necessary to carry out some form of marginalization over the unknown VULF parameters.

The derived constraints on VULF dark matter presented in Ref. [13] take advantage of the signal model presented in Eq. (20). Any DM signal with frequency f_ϕ below the $1/T$ resolution will be upconverted to the 1/day frequency (f_E) given by Earth's rotation. Thus, instead of trying to resolve frequencies below the $1/T$ resolution, we constrain all frequencies below that threshold by looking only at the f_E bin that is within the detection bandwidth. The constraint levels off (becomes constant) for all frequencies below $\sim 1/(25T)$ when $2\pi f_\phi T \approx 0$ and the signal amplitude is dominated by the $|\sin\theta|$ distribution. The height of this constant level is determined by the chosen confidence level, as there are a small range of phases that give vanishing signals for arbitrarily large coupling.

This approach can be used for all pseudoscalar (“wind”-type) experiments that can resolve the f_E frequency. We additionally note that scalar searches (for which this upconversion does not occur) which are sensitive to offsets (the zero-frequency component) can also draw similar constraints below the $1/T$ frequency threshold. There is a caveat that any signal present at the f_E frequency would not allow determination of the actual f_ϕ , only that it is smaller than $1/T$. Additionally, differentiating systematic errors from potential VULF dark matter signals is difficult for upconverted frequencies; one approach would be to confirm the expected yearly modulation in the event of a detection.

II. COHERENCE TIME

Another topic is the presence of various definitions of coherence time used throughout the literature. The most common definition used is $\tau_c \equiv (f_c v_{\text{vir}}^2/c^2)^{-1}$ and is the one used in the paper. It is a lower bound derived by considering our motion through the spatial gradients of the field [18, 19] given by λ , the De Broglie wavelength,

$$\tau_c \sim \lambda/v_{\text{vir}} = \frac{h}{m_\phi v_{\text{vir}}^2} = (f_c v_{\text{vir}}^2/c^2)^{-1} \approx 10^6/f_c = 1s \left(\frac{\text{MHz}}{m_\phi} \right) \quad (21)$$

where we have used the Compton frequency $f_c = m_\phi c^2/h$ and $v_{\text{vir}} \approx 10^{-3}c$. However, some definitions differ by factors around $\sim 2\pi$ [20]. A factor of 2 can occur from using the kinetic energy $mv^2/2$ instead of mv^2 as in Ref. [18, 19] or in using 10^6 as the quality factor and corresponding definition of coherence time.

These differences in coherence time do not have a significant effect on the results in this paper nor previous published constraints. The strongest effect would be the shift of the upper bound on m_a of the CASPER-ZULF-Sidebands constraint. Since the experiment is incoherently averaging past this point the constraint significantly weakens and was not reported. In addition, the fuzzy definition of coherence time also depends on the relative velocity, making it a distributed quantity.

In regards to this upper bound, a potentially more precise T_{max} can be derived (where the regime discussed in this paper would go from $T \ll \tau_c$ to $T \ll T_{\text{max}}$) considering the lineshape derived in Ref. [20]. Using the derived full width at half maximum $\Delta\omega \approx 2.5/\tau_c$ and setting equal to the DFT frequency step $\delta\omega = 2\pi/T$ gives $T_{\text{max}} \approx 2\pi\tau_c/2.5$, or with the definition of coherence time used in this paper: $T_{\text{max}} \approx \tau_c/2.5$. Thus it is safe to assume the data from the experiments shown are all in the $T \ll T_{\text{max}}$ regime, regardless of the definition of coherence time.

III. RAYLEIGH DISTRIBUTION

As shown in Eq. (1), Φ_0 is the observed amplitude, and in the case of total interrogation time being much less than the field's coherence time, $T \ll \tau_c$, the only amplitude observed during a measurement. One can relate the local dark matter density ρ_{DM} to the field's energy density $\Phi_0^2 f_\phi^2/2 = \rho_{\text{DM}}$ as done for example by Graham in Ref. [18]. The problem with this is that Φ_0 is actually a Rayleigh distributed value, thus the correct expression is

$$\langle \Phi_0^2 \rangle \frac{c^2 m_\phi^2}{2\hbar^2} = \rho_{\text{DM}}. \quad (22)$$

We can define Φ_{DM} as the value satisfying Eq. (22)

$$\Phi_{\text{DM}} = \sqrt{\langle \Phi_0^2 \rangle} = \frac{\sqrt{2\rho_{\text{DM}}}}{m_\phi}, \quad (23)$$

analogous to previous assumptions of $\Phi_0 = \Phi_{\text{DM}}$ in the deterministic approach.

Using Eq. (22) we can solve for the required σ of the Rayleigh distribution $p(\Phi_0)$.

$$\begin{aligned} \langle \Phi_0^2 \rangle &= \int \Phi_0^2 p(\Phi_0) d\Phi_0 = \int_0^\infty \frac{\Phi_0^3}{\sigma^2} \exp\left(-\frac{\Phi_0^2}{2\sigma^2}\right) d\Phi_0 = \Phi_{\text{DM}}^2 \\ &\implies \sigma = \Phi_{\text{DM}}/\sqrt{2} \text{ thus,} \\ p(\Phi_0) &= 2 \frac{\Phi_0}{\Phi_{\text{DM}}^2} \exp\left(-\frac{\Phi_0^2}{\Phi_{\text{DM}}^2}\right). \end{aligned} \quad (24)$$

Note that the average value of this distribution $\langle \Phi_0 \rangle = \Phi_{\text{DM}}\sqrt{\pi}/2$ is not simply Φ_{DM} . Approximately 63% of given field realizations will have an amplitude smaller than Φ_{DM} . The distribution compared to Φ_{DM} is shown in Fig. 1.

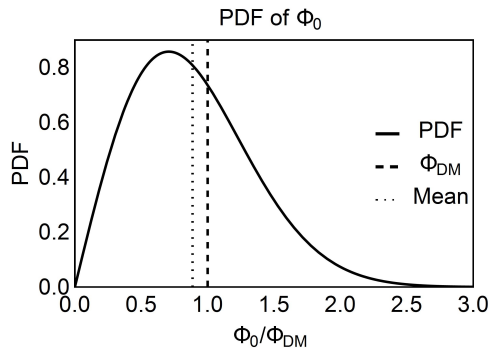


FIG. 1: Rayleigh distribution given by Eq. (24).

-
- [1] R. D. Cousins, *American Journal of Physics* **63**, 398 (1995).
 - [2] J. Heinrich, in *PHYSTAT LHC Workshop on Statistical Issues for LHC Physics, PHYSTAT 2007 - Proceedings* (2008).
 - [3] L. Lyons, *The Annals of Applied Statistics* **2**, 887 (2008).
 - [4] I. Narsky, *Nuclear Instruments and Methods in Physics Research Section A: Accelerators, Spectrometers, Detectors and Associated Equipment* **450**, 444 (2000).
 - [5] A. L. Read, Cern-Open (2000).
 - [6] A. Derevianko, *Phys. Rev. A* **97**, 042506 (2018), arXiv:1605.09717.
 - [7] S. Knirck, A. J. Millar, C. A. O'Hare, J. Redondo, and F. D. Steffen, *Journal of Cosmology and Astroparticle Physics* **2018**, 051 (2018), arXiv:1806.05927.
 - [8] J. Aalbers, K. Dundas Morà, and B. Pelszers, “JelleAalbers/blueice: v1.0.0-beta.2,” (2019).
 - [9] E. T. Jaynes, in *Maximum-Entropy and Bayesian Spectral Analysis and Estimation Problems*, edited by C. R. Smith and G. J. Erickson (D. Reidel Publishing Company, Dordrecht, Holland, 1987) pp. 1–37.
 - [10] Strictly speaking one needs to use Jeffrey’s (scale invariant prior) $\propto 1/\gamma$ here, but the previous analyses do not use it. We employ a sufficiently broad uniform prior for γ for consistency with the literature.
 - [11] J. Conrad, “Statistical issues in astrophysical searches for particle dark matter,” (2015).
 - [12] M. Tanabashi, K. Hagiwara, K. Hikasa, K. Nakamura, Y. Sumino, F. Takahashi, J. Tanaka, K. Agashe, G. Aielli, C. Amsler, *et al.*, “Review of Particle Physics,” (2018), arXiv:0601168 [astro-ph].

- [13] T. Wu, J. W. Blanchard, G. P. Centers, N. L. Figueroa, A. Garcon, P. W. Graham, D. F. J. Kimball, S. Rajendran, Y. V. Stadnik, A. O. Sushkov, A. Wickenbrock, and D. Budker, *Physical Review Letters* **122**, 191302 (2019), [arXiv:1901.10843](#).
- [14] A. Garcon, J. W. Blanchard, G. P. Centers, N. L. Figueroa, P. W. Graham, D. F. Jackson Kimball, S. Rajendran, A. O. Sushkov, Y. V. Stadnik, A. Wickenbrock, T. Wu, and D. Budker, *Science Advances* **5**, eaax4539 (2019), [arXiv:1902.04644](#).
- [15] E. G. Adelberger and W. A. Terrano, *Physical Review Letters* **123**, 169001 (2019).
- [16] T. Wu, J. W. Blanchard, G. P. Centers, N. L. Figueroa, A. Garcon, P. W. Graham, D. F. J. Kimball, S. Rajendran, Y. V. Stadnik, A. O. Sushkov, A. Wickenbrock, and D. Budker, *Physical Review Letters* **123**, 169002 (2019).
- [17] W. A. Terrano, E. G. Adelberger, C. A. Hagedorn, and B. R. Heckel, *Physical Review Letters* **122**, 231301 (2019), [arXiv:1902.04246](#).
- [18] P. W. Graham and S. Rajendran, *Physical Review D - Particles, Fields, Gravitation and Cosmology* **88**, 1 (2013), [arXiv:arXiv:1306.6088v2](#).
- [19] D. Budker, P. W. Graham, M. Ledbetter, S. Rajendran, and A. O. Sushkov, *Physical Review X* **4**, 021030 (2014), [arXiv:1306.6089](#).
- [20] A. Derevianko, *Physical Review A* **97**, 042506 (2018), [arXiv:1605.09717](#).